Measuring the Orbital Angular Momentum of Light Based on Optical Differentiation

Liang Fang, Lan Luo, Rujin Zhao, and Bo Liu

***Abstract*—The utilization of orbital angular momentum (OAM) in light for information encoding is a promising avenue, as it exhibits resilience against environmental disturbances. However, the direct detection of OAM poses a significant challenge due to beam distortion during transmission, which ultimately limits the practical application of OAM-based optical communication. We propose an environmentally friendly and intuitive detection method based on optical differentiation using a weak-measurement system. Optical differential measurements were conducted on Laguerre-Gaussian beams (L-G beams) with $l = 5$ and $l = 8$ to validate the feasibility of this approach. This approach mitigates the impact of disturbances on OAM measurement, enabling direct detection through a simplified system, which serves as a valuable reference for utilizing OAM as an information carrier in free-space optical communication.**

***Index Terms*—Imaging, optical differentiation, quantum detection.**

I. Introduction

THE vortex beams carrying the OAM have performed impressively in many fields such as optical communication, transmission and manipulation since Allen and coworkers' seminal paper [1]. Owing to the OAM, a higher degree of freedom is provided to enhance the capability of optical communication [2], [3]. With the development of optical communication, free-space optical communication becomes the focus owing to the flexibility, security, and large-signal bandwidth [4], [5]. Compared with the traditional gauss beam, the vortex beams exhibit anti-disturbance ability when they propagate though the free-space [6], [7]. With the above characteristics, the vortex beams show an excellent capability of information dissemination [8], [9]. Therefore, the free-space optical communication based vortex beams becomes the one of the mainstream applications [9], [10]. But the OAM detection at the receiver side is difficult to make, because of the perturbation of the OAM states in transmission [11], [12], [13].

Manuscript received 24 April 2023; revised 5 June 2023; accepted 6 June 2023. Date of publication 16 June 2023; date of current version 11 August 2023. This work was supported in part by the Laboratory Innovation Foundation of the Chinese Academy of Science, in part by Sichuan Outstanding Youth Science and Technology Talent Project under Grant 2022JDJQ0027, and in part by the CAS "Light of West China" Program and Special support for talents from the Organization Department of Sichuan Provincial Party Committe. *(Corresponding author: Bo Liu.)*

The authors are with the Institute of Optics and Electronics, Chinese Academy of Sciences, Chengdu 610209, China, and also with the Key Laboratory of Science and Technology on Space Optoelectronic Precision Measurement, Chinese Academy of Sciences, Chengdu 610209, China (e-mail: fangl@ioe.ac.cn; naluol@163.com; zrj0515@163.com; boliu@ioe.ac.cn).

Digital Object Identifier 10.1109/JPHOT.2023.3285226

Many researches have been proposed to measure the OAM of the vortex beams. Assessment established on field date [14], [15], [16], indirect detection through the effects induced by vortex beams [17], [18], [19] and beam-restoring using holographic technology [20], [21] are three main kinds of OAM detection. Also belong to the three kinds of representative detection work, Wang et al. [15] proposed a convolutional neural network named RoamN-CNN to identify the OAM of two orthogonal polarized vortex beams from the speckle pattern. Genevet et al. [22] put forward a method based on the principle of holography realized the detection of the OAM of light with plasmonic photodiodes. Zhao et al. [23] propose a multipoint interferometer (IMI) to detect the vortex beams and demonstrate that the far-field interference patterns using such a method can be used to measure the vortex beams with high topological charge. These works have made a significant contribution in this area. But lots of computation, simulation and the short of restoring beams transported in disturbed space leave us with problems. And the detection after transmission disturbance is not fully considered. They usually consider the combination of adaptive and other ways to recover the phase before measurement [24], [25], [26] which makes the detection systems become complicated and lose detection efficiency.

Here, we put forward an OAM detection method without any beam compensation mechanism by optical differentiation on the special phase distribution of vortex beams, the numbers of phase jump corresponding to the OAM. We utilize birefringent crystals (BCs) to induce spatial displacement and achieve phase differentiation of vortex beams by constructing an imaginary weak value with a weak-measurement system. In our experiment, we detect Laguerre-Gaussian beams of varying orders, demonstrating the continued utility of this detection scheme even in cases of random perturbative propagation. This underscores the superiority of our method for detecting orbital angular momentum (OAM).

II. Theory

In the previous work, the idea of constructing weak values has been proposed [27], [28], [29] and it is adopted in the optical differentiation with weak measurements which has been described thoroughly [27], [30], [31], [32], [33], [34], [35], [36]. Through differentiation with the phase of a Gaussian beam, the feasibility of the theory is proved. Thinking the vortex beam has abrupt change of phase because the phase factor $e^{il\theta}$. l is the order of vortex beam (the OAM of vortex beam) and θ is azimuth angle. The presence of phase breaks makes the detection possibly. We

construct a measurement scheme with pre- and post-selections, in which the pre- and post-selected states are respectively chosen as $|\varphi_i\rangle$, $|\varphi_f\rangle$ [37], [38]. The wave function of vortex beam here can be expressed as ϕ (the probes in weak-measurement system). The unitary transformation of the coupling system and probe takes the following form

$$U = \exp(-i\gamma \hat{A} \otimes \hat{p}) \tag{1}$$

Weak coupling strength γ is defined by the spatial shift of BC. $\hat{A}$ is the operator of observable measurement of the system. $\hat{p}$ denotes the operator of momentum p. The output state of the whole system can be expressed as

$$|\Phi_{\text{output}}\rangle = \langle\varphi_f|U|\phi\rangle \otimes |\varphi_i\rangle \tag{2}$$

When the γ is sufficiently weak, (1) can be expanded and taken as follows

$$U \simeq 1 - i\gamma \hat{A} \otimes \hat{p} \tag{3}$$

For convenience later, we're going to discuss in 1D contribution on the x axis. The probability distribution of detecting the wave function in coordinate space can be expressed as

$$\begin{aligned} \Phi(x) &= |\langle x \mid \Phi_{\text{output}}\rangle|^2 \\ &\simeq |\langle\varphi_f \mid \varphi_i\rangle \phi(x) (1 - i\gamma A_w p_w)|^2 \end{aligned} \tag{4}$$

Where the $A_w = \frac{\langle\varphi_f|\hat{A}|\varphi_i\rangle}{\langle\varphi_f|\varphi_i\rangle}$ is defined as the system weak value. And we generate a special weak value $p_w = \frac{\langle x|\hat{p}|\phi\rangle}{\langle x|\phi\rangle} = -i\frac{1}{\phi(x)}\frac{\partial\phi(x)}{\partial x}$. The system weak value A_w is defined only by the pre- and post- selections. When the pre- and post-selected states are nearly orthogonal $\langle\varphi_f|\varphi_i\rangle \approx 0$, the A_w tends to be sufficiently large. Although the γ is sufficiently weak, we can also keep the second term in (4). For the vortex beam, we can express the wave function as $\phi(x) = a(x)e^{ib(x)}$. Rewrite the (4) as

$$\Phi(x) = \left|\langle\varphi_f \mid \varphi_i\rangle \left[a(x) - \gamma A_w \frac{\partial a(x)}{\partial x} - i\gamma a(x) A_w \frac{\partial b(x)}{\partial x}\right]\right|^2 \tag{5}$$

It worth noting that the last two terms include the differentiation of amplitude and phase respectively and they correspond to the real and imaginary terms. We can use diverse post-selected states to contrast pure imaginary or real weak values to acquire the differentiation of phase or amplitude. In our experiment, By contrasting two pure imaginary weak value $A_w = \pm i\tau$ (τ is a positive real number) to generate corresponding probability distributions as follows

$$\Phi_{\pm}(x) = \left|\langle\varphi_f \mid \varphi_i\rangle a(x) \left[1 \pm i\gamma\tau \frac{\partial b(x)}{\partial x}\right]\right|^2 \tag{6}$$

The differentiation of phase can be exacted

$$\Phi_+(x) - \Phi_-(x) = |\langle\varphi_f \mid \varphi_i\rangle|^2 4\gamma\tau a^2(x) \frac{\partial b(x)}{\partial x} \tag{7}$$

From (7), we can find that by measuring $\Phi_{\pm}(x)$ in output port and subtracting them, we can get the signal that is proportional to the phase's differentiation. Choosing the direction of differentiation along with the y axis, we can acquire the 2-D differentiation.

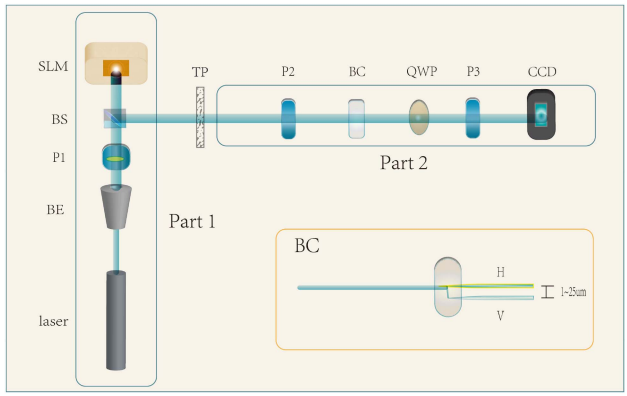

Fig. 1. Experiment diagram. Part 1 is contracted for vortex beam generation[The amplification beam expander, polarizer 1 (P1), Beam splliter (BS), spatial light modulator (SLM)]; Part 2 is contracted for detection[Turbulence plate (TP) is only used in the randomly perturbative transmission direction. The pre-selected state is determined by polarizer 2 (P2). The post-selected states are determined by polarizer 3 (P3) and a quarter-wave plate (QWP). The birefringent crystal (BC) is used to generate a shift dx. The output beam is collected by the CCD camera].

III. Experiment and Simulations

The experiment scheme is shown in Fig. 1, where the illustration in Fig. 1 shows the details of BC. The L-G beams is generated in the Part1 and the weak-measurement system is displayed in the Part2. Note that the design of Part2 is different in the two experiments which is embodied in the distance of propagation and the usage of turbulence plate. We use the spatial light modulator (SLM) to acquire L-G beams with different OAM. In the Part2, we contract the pre- and post-selection with P1 and a combination of quarter-wave plate (QWP) and P2. The pre-selection state can be expressed as $|\varphi_i\rangle = \frac{1}{\sqrt{2}}(|H\rangle + |V\rangle)$ which corresponds to the +45^o linear polarization. The post-selection states $|\varphi_{f\pm}\rangle = \frac{1}{\sqrt{2}}[\exp(\mp i\sigma|H\rangle - \exp(\pm i\sigma)|V\rangle]$ are constructed by the QWP and P2 with polarization at $(-45^o \pm \sigma)$, where the σ is assigned to an angle from -45^o. In the experience, we choose the tiny angle σ as 3^o. The birefringent crystal (BC) is placed between the pre- and post- selection, providing a small displacement dx of the beam in the x direction, as shown in Fig. 1. The L-G beam with the order of l can be expressed as in the cylindrical coordinates [39], [40]

$$\phi(r, \theta, z) = L^{|l|}(r, z)e^{i(l\theta+\xi)} \tag{8}$$

Here, $L(r, z)$ is amplitude term, which is no deal with the phase term. $\xi = (l + 2p + 1)\arctan(\frac{z}{f}) - k(z + \frac{r^2}{2R})$, l is angular quantum numbers, p is radial quantum numbers, $f = \frac{\pi\omega_0^2}{\lambda}$ is Rayleigh length (ω_0 is donated to beam waist radius and λ is donated to the wavelength) and R=z+$\frac{f^2}{z}$. We can acquire the distribution of amplitude $I_{LG} \propto |L^{|l|}(r, z)|^2$ which is constant with a certain order l, r and z. The distribution of phase along the x axis can be expressed as $b(x) = l\theta(x) + \xi$. The (7) can be rewritten simply as

$$\Phi_+(x) - \Phi_-(x) \propto a^2(x) \frac{\partial b(x)}{\partial x} \tag{9}$$

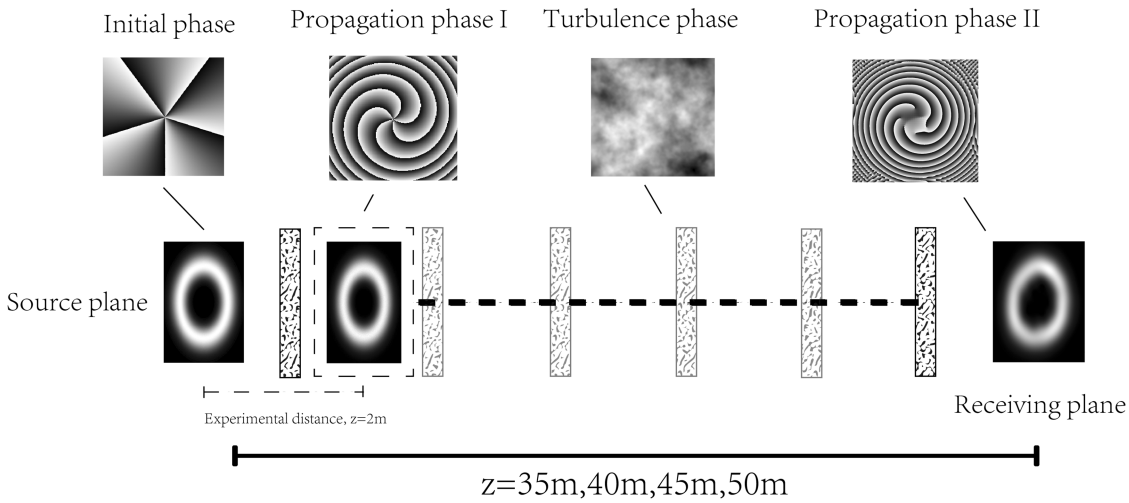

Fig. 2. Propagation diagram of a vortex beam with $l = 5$ in randomly atmospheric turbulence.The initial phase, propagation phase I and propagation phase II corresponds to the vortex phase in the case of nonperturbative situation, the vortex phase when the simulated distance is the experimental distance and the vortex phase after propagation distance z, respectively.

Where the $a^2(x)$ is the distribution of amplitude I_{LG} that is constant. Through the formulate, we can find that compared with Gaussian beams, there is one more phase factor $l\theta(x)$ in the phase term, and it will donate a phase hits. Here's the thing to note that the phase hits of vortex beams are not strictly from 2π to 0, but from 2π to $0 + \delta, \delta \in (0, 2\pi)$. We carry out the analytical simulation as shown in Fig. 2. We consider a propagation model of vortex beam with $l = 5$ under atmospheric random disturbance to prove the detection method is universal. Set the beam waist diameter of the vortex beam to $\omega_0 = 2.0 \times 10^{-3}$ m and the turbulence structure constant $Cn^2 = 2.0 \times 10^{-12}$ which is contributed to the intensity of the phase perturbation [41], [42], [43]. The vortex beam $l = 5$ is modulated at the source plane, and set six random phase disturbance plates at upper spacing along the propagation path. The initial phase, propagation phase I, and propagation phase II correspond to the vortex phase in non-perturbative situations, the vortex phase when simulated distance equals experimental distance $z = 0.1$ m, 2 m, and the vortex phase after propagating a distance $z = 35$ m, 40 m, 45 m, 50 m respectively. [7], [44], [45]. The modulated results is presented in the Fig. 3, which is the differential of the vortex phase with $l = 5$ and $l = 8$ along the x and y directions in the case of nonperturbative situation. The loaded phase maps are shown in Fig. 3(a) and (e). Through the loaded phase modulating, we can get the intensity of vortex beams shown as the Fig. 3(b) and (e). The differential results of $l = 5$ and $l = 8$ are listed in Fig. 3(c), (d) and (f), (g) respectively. As shown in the figure, We make the differential in x and y direction, through which we can get the OAM of the vortex beams. The same as the nonperturbative one, we make a calculation of the situation after randomly perturbative transmission and the propagation distance was set to z = 2 m. The results are presented in the Fig. 4. As the Fig. 4(a), (b) and (e), (f) show that the phase of the vortex beams is bent during the propagation and the intensity of the vortex beams is uneven. The differential results of $l = 5$ and $l = 8$ listed in Fig. 4(c), (d) and (f), (g) respectively which are

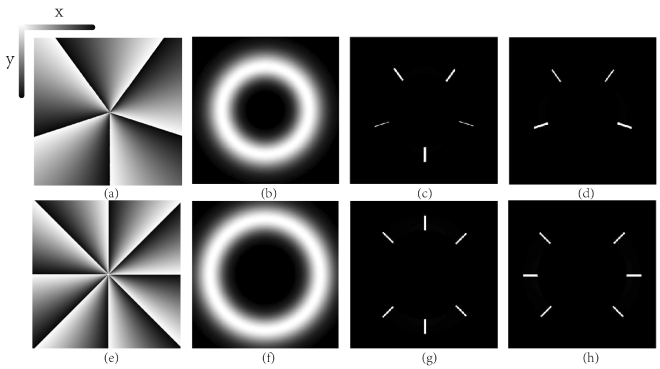

Fig. 3. The differentiation of vortex phase in the x and y directions with $l = 5$ and $l = 8$ without randomly perturbative propagation. (a), (e) The phase loaded on the SLM. (b), (f) The intensity of the vortex beams with $l = 5$ and $l = 8$. (c), (d) Differentiation of vortex phase in x and y directions for a vortex beam with $l = 5$. (g), (h) Differentiation of vortex phase in x and y directions for a vortex beam with $l = 8$.

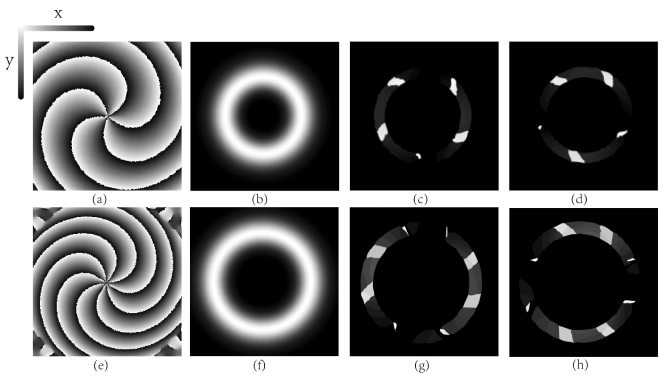

Fig. 4. Differentiation of vortex phase in the x and y directions with $l = 5$ and $l = 8$ with randomly perturbative propagation, z = 2 m. (a), (e) The vortex phase after randomly perturbative progragation. (b), (f) The intensity of the vortex beams with $l = 5$ and $l = 8$. (c), (d) Differentiation of vortex phase in x and y directions for a vortex beam with $l = 5$. (g), (h) Differentiation of vortex phase in x and y directions for a vortex beam with $l = 8$.

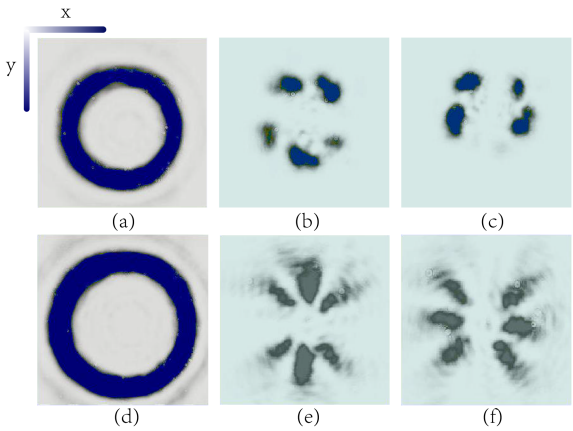

Fig. 5. Experimental results without randomly perturbative propagation. (a), (d) the indensity of vortex beams with $l = 5$ and $l = 8$. (b), (c) Differentiation in x and y directions for a vortex beam with $l = 5$. (e), (f) Differentiation in x and y directions for a vortex beam with $l = 8$.

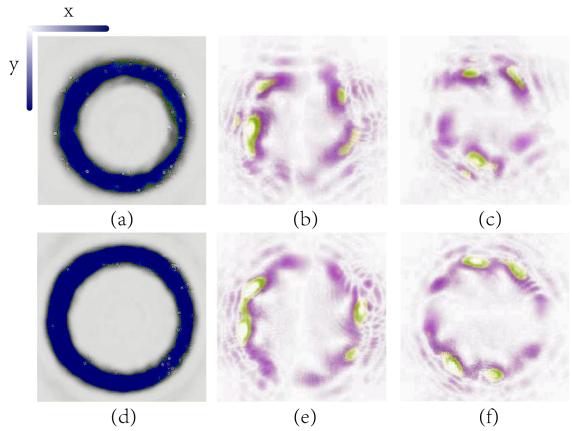

Fig. 6. Experimental results with randomly perturbative propagation, z = 2 m. (a), (d) the indensity of vortex beams with $l = 5$ and $l = 8$. (b), (c) Differentiation in x and y directions for a vortex beam with $l = 5$. (e), (f) Differentiation in x and y directions for a vortex beam with $l = 8$.

greatly different from the nonperturbative one. With the propagation, the vortex beams are affected by random disturbance and the phase is interfered. The curved phases of the vortex beams can be detected with the methods and the OAM can be acquired obviously. It is certain that the vortex beam will lose its original properties with distance. The calculated results are well correspond with the above theory and the feasibility of this method is well verified.

IV. Results

For experimental demonstration of the above proposed detection method, We build the experimental setup as mentioned above to detect vortex beams with $l = 5$ and $l = 8$ in the case of nonpropagation and randomly perturbative propagation respectively. Set the experimental parameters corresponding to the theoretical simulation presented in the Figs. 3 and 4 as the waist diameter to $\omega_0 = 2.0 \times 10^{-3}$ m and transmission distance to $z = 0.1$ m which can be regarded as nonpropagation and $z = 2$ m. We consider a transparent glass plate coated randomly as the random disturbance plate. The experimental results of nonpropagation are presented in the Fig. 5, where Fig. 5(a) and (d) show the intensity of the vortex beams with $l = 5$ and $l = 8$, Fig. 5(b) and (c) show the differential results of vortex beams with $l = 5$ on x and y axis, Fig. 5(d) and (f) show the differential results of vortex beams with $l = 8$ on x and y axis respectively. By differentiating the vortex beam in the x and y directions, we can obtain the differentiation in the whole space, so as to obtain the accurate order of the vortex beam. In order to verify the detection method is also useful in the case of randomly perturbative propagation, we provide conditions for vortex beams to propagate to simulate propagation of vortex beams in the space of random disturbance. The Fig. 6(a) and (d) show the indentity of vortex beams with $l = 5$ and $l = 8$ through propagation respectively. The differential results are listed in the Fig. 6(b), (c) and (e), (f) which are presented as the differentiation of $l = 5$ and $l = 8$. The phase of the vortex beam bends during propagation, which makes it

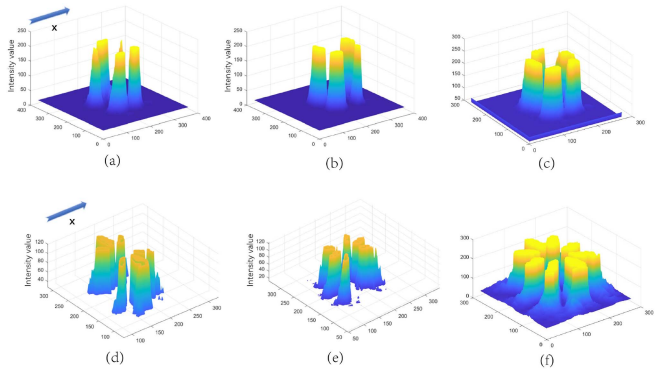

Fig. 7. 3D reconstruction of phase differential results with $l = 5$ and $l = 8$. (a), (d) The differential in the x direction with $l = 5$ and $l = 8$. (b), (e) The differential in the y direction with $l = 5$ and $l = 8$. (c), (f) The sum of the differential results in x and y directions.

difficult to detect OAM accurately. The method based on the optical differentiation can filter out the phase of disturbance and detect OAM effectively combined with weak measurements.

To enhance the visibility of the orbital angular momentum (OAM) carried by vortex beams, we perform 3D reconstruction on the differential results of vortex beams with $l = 5$ and $l = 8$. As shown in Fig. 7, We can easily acquire the OAM of the vortex beam with $l = 5$ and $l = 8$ corresponding to the nonperturbative one. From the reconstructed 3D pictures, we can more clearly reflect the different light intensity caused by the different differential direction and phase distribution. Fig. 7(a) and (d) show the differential of the vortex beam with $l = 5$ and $l = 8$ in the x direction, from which we can clearly see that the abrupt phase distribution near the differential direction corresponds to the bar column with smaller intensity value. We also analyze the results of the differentiation in the y direction shown as the Fig. 7(b) and (e). By simply adding the differential results in the x and y directions, we can obtain the OAM of the vortex beams obviously presented as the Fig. 8(c) and (f).

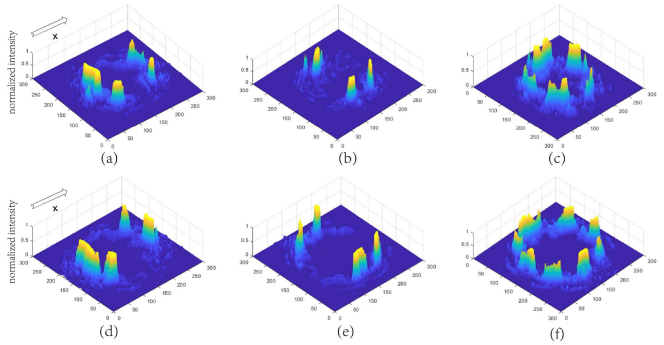

Fig. 8. 3D reconstruction of phase differential results with $l = 5$ and $l = 8$ after randomly perturbative propagation. (a), (d) The differential in the x direction with $l = 5$ and $l = 8$. (b), (e) The differential in the y direction with $l = 5$ and $l = 8$. (c), (f) The sum of the differential results in x and y directions.

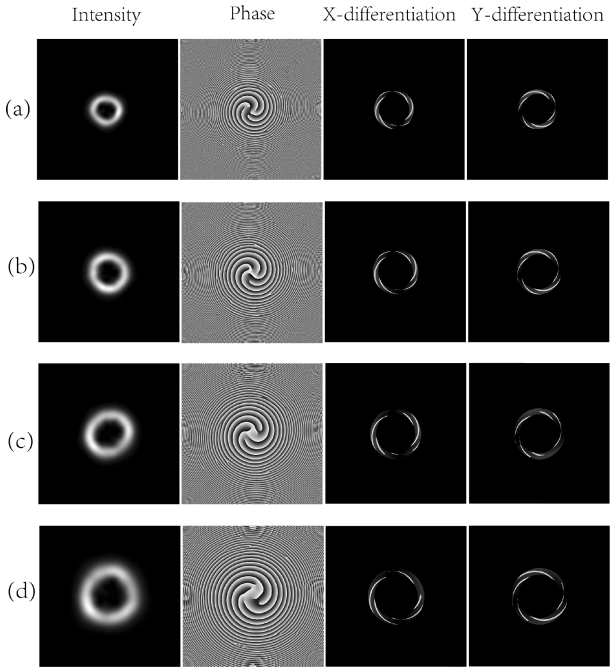

Fig. 9. Calculated results with different propagation distances. Corresponding distances of (a-b) are $z = 35$ m, $z = 40$ m, $z = 45$ m, $z = 50$ m. The lists of pictures are presented as the intensity, vortex phase, differential detection in x and y directions of the vortex beam.

The reconstruction of the 3D images provide a clearer basis for the analysis of the results. Considering the normalization of light intensity, we carry out the same 3D reconstruction for the differential results of $l = 5$ and $l = 8$ vortex beams after randomly perturbative propagation shown as the Fig. 8. We can clearly identify the OAM of the vortex beams, which is consistent with the theoretical calculation. From the Figs. 7 and 8, we can find that the ineffectual intensity of background and stray light is greatly compressed, which is owing to differential methods based on the weak measurements [46], [47], [48]. We have experimentally measured the vortex beams with $l = 5$ and $l = 8$ without propagating disturbance and after propagating disturbance, which proves the feasibility of the theory.

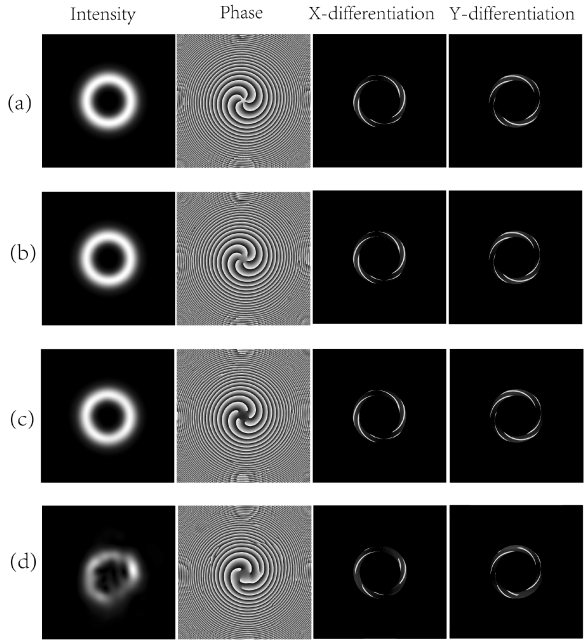

Fig. 10. Calculated results with different turbulence intensity disturbances. The corresponding turbulence structure constant of (a-b) are $Cn^2 = 2.0 \times 10^{-17}, Cn^2 = 2.0 \times 10^{-15}, Cn^2 = 2.0 \times 10^{-13}, Cn^2 = 2.0 \times 10^{-11}$. The lists of pictures are presented as the intensity, vortex phase, differential detection in x and y directions of the vortex beam.

V. Discussions and Conclusions

In addition to the aforementioned simulations and experiments, we conducted further assessments of the detection method's performance through additional simulations. As listed in Fig. 9(a)-(d), the pictures show the intensity, phase and differential results of vortex beams with $l = 5$, which propagate different distances $z = 35$ m, 40 m, 45 m and 50 m with the same turbulence intensity disturbance corresponding to $Cn^2 = 2.0 \times 10^{-12}$. We also simulate the detection of vortex beams propagation with $l = 5$ through turbulence of varying intensities at a fixed distance $z = 50$, shown in Fig. 10(a)-(d). The Cn^2 numerical values, are values that vary: 2.0×10^{-17}, 2.0×10^{-15}, 2.0×10^{-13} and 2.0×10^{-11}, are considered to cover strong, moderate, and weak turbulence [7], [41], [42], [43], [44], [45]. The simulation results show that, as depicted in Fig. 9, the phase of the vortex beam exhibits increasingly chaotic behavior with propagation distance under strong perturbations. Within a certain range of propagation distances, our detection method yields clear and direct OAM measurement results shown as the Fig. 9(a)-(c). However, with increasing propagation distance as depicted in Fig. 9(d), the acquired detection outcomes may become less intuitive and lead to inaccurate OAM measurement. As depicted in Fig. 10(a)-(c), the proposed method is effective in obtaining clear detection results when the turbulence intensity is insufficient to induce chaotic phase of vortex beam. However, as illustrated Fig. 10(d), inaccurate test outcomes may arise due to severe chaos of vortex phase under high turbulence intensity, which renders it unsuitable for relevant applications [45], [49]. By combining the simulation results of different propagation distances mentioned above, as illustrated in Fig. 9, it can be

inferred that our detection method is capable of effectively detecting the OAM of vortex beams transmitted through free space without being affected by destructive turbulence. Moreover, for conventional strong turbulence, this detection scheme remains feasible within a certain range of propagation. According to the calculated and experimental results, in the effective propagation ranges of the vortex beams, the detection scheme is feasible and reliable which can be well used in optical communication based on vortex beams. In this paper, we propose a detection method for single OAM and demonstrate its feasibility through experiments and simulations. Furthermore, we show that the method can be adapted to disturbance transmission. Additionally, the utilization of this technique for multiplexed OAM detection exhibits great potential and interest, which be served as a focal point for future research to address current issues of signal crosstalk and noise interference caused by turbulence disturbances [26], [50], [51]. This method offers an intriguing avenue for distinguishing between various vortex modes [52]. The efficacy of the L-G model has been demonstrated in this study, and our proposed detection approach exhibits high sensitivity towards the phase term $e^{il\theta}$. Based on the concept of differentiation, we can propose temporal differentiation to analyze the phase term associated with propagation direction. This allows for clear reflection of vortex beams with different modes in this term, enabling separate measurement and further study of these modes in future research.

In conclusion, we conducted optical differential measurements on OAM beams with $l = 5$ and $l = 8$ under non-propagating and randomly perturbed propagation conditions. Benefiting from the capability of suppressing background noise in weak measurement systems, we are able to clearly obtain the OAM. The detection methods effectively mitigate the impact of background light and stray light, enabling the acquisition of orbital angular momentum (OAM) of vortex beams despite undergoing random perturbations during propagation.The validity of an optical differentiation-based system for detecting angular momentum has been fully confirmed. This detection method is anticipated to facilitate the advancement of optical communication applications based on vortex beams and provide a valuable reference for addressing intricate issues in this field.

REFERENCES

[1] L. Allen, M. W. Beijersbergen, R. Spreeuw, and J. P. Woerdman, "Orbital angular momentum of light and the transformation of Laguerre-Gaussian laser modes," *Phys. Rev. A*, vol. 45, 1992, Art. no. 8185.

[2] A. Nicolas, L. Veissier, L. Giner, E. Giacobino, D. Maxein, and J. Laurat, "A quantum memory for orbital angular momentum photonic qubits," *Nature Res.*, vol. 8, no. 3, pp. 234–238, 2014.

[3] D. Bacco, D. Cozzolino, B. Da Lio, Y. Ding, K. Rottwitt, and L. K. Oxenløwe, "Quantum communication with orbital angular momentum," in *Proc. 22nd Int. Conf. Transparent Opt. Netw.*, 2020, pp. 1–4, doi: 10.1109/ICTON51198.2020.9203023.

[4] M. A. Khalighi and M Uysal, "Survey on free space optical communication: A communication theory perspective," *IEEE Commun. Surveys Tuts.*, vol. 16, no. 4, pp. 2231–2258, Fourthquarter 2014.

[5] V. W. S. Chan, "Free-space optical communications," *J. Lightw. Technol.*, vol. 24, no. 12, pp. 4750–4762, Dec. 2006.

[6] W. B. Wang, R. Gozali, L. Shi, L. Lindwasser, and R. R. Alfano, "Deep transmission of Laguerre–Gaussian vortex beams through turbid scattering media," *Opt. Lett.*, vol. 41, no. 9, pp. 2069–2072, May 2016. [Online]. Available: https://opg.optica.org/ol/abstract.cfm?URI=ol-41-9-2069

[7] T. Wang, J. Pu, and Z. Chen, "Beam-spreading and topological charge of vortex beams propagating in a turbulent atmosphere," *Opt. Commun.*, vol. 282, no. 7, pp. 1255–1259, 2009. [Online]. Available: https://www.sciencedirect.com/science/article/pii/S0030401808012881

[8] J. Wang et al., "Terabit free-space data transmission employing orbital angular momentum multiplexing," *Nature Res.*, vol. 6, no. 7, pp. 488–496, 2012.

[9] G. Gibson et al., "Free-space information transfer using light beams carrying orbital angular momentum," *Opt. Exp.*, vol. 12, no. 22, pp. 5448–5456, 2004.

[10] J. Wang, "Advances in communications using optical vortices," *Photon. Res.*, vol. 4, no. 11, 2016, Art. no. B14. [Online]. Available: https://www.researching.cn/articles/OJ778679a80a3f98ce

[11] G. Gbur and R. K. Tyson, "Vortex beam propagation through atmospheric turbulence and topological charge conservation," *JOSA A*, vol. 25, no. 1, pp. 225–230, 2008.

[12] X.-L. Ge, B.-Y. Wang, and C.-S. Guo, "Evolution of phase singularities of vortex beams propagating in atmospheric turbulence," *JOSA A*, vol. 32, no. 5, pp. 837–842, 2015.

[13] G. Zhou, L. Zhang, and G. Ru, "Vectorial structural properties of a Gaussian vortex beam in the far-field," *Laser Phys.*, vol. 25, no. 12, Oct. 2015, Art. no. 125001. [Online]. Available: https://dx.doi.org/10.1088/1054-660X/25/12/125001

[14] T. Yu, H. Xia, W. Xie, and Y. Peng, "Orbital angular momentum mode detection of the combined vortex beam generated by coherent combining technology," *Opt. Exp.*, vol. 28, no. 24, pp. 35795–35806, 2020.

[15] Z. Wang et al., "Recognizing the orbital angular momentum (OAM) of vortex beams from speckle patterns," *Sci. China Phys., Mechanics Astron.*, vol. 65, no. 4, pp. 1–7, 2022.

[16] M. J. Padgett, M. Lavery, G. Berkhout, J. Courtial, and M. Beijersbergen, "Measuring the orbital angular momentum of light," *Proc. SPIE*, vol. 7950, 2011, Art. no. 79500E, doi: 10.1117/12.876119.

[17] S. M. Mohammadi et al., "Orbital angular momentum in radio: Measurement methods," *Radio Sci.*, vol. 45, no. 04, pp. 1–14, 2010.

[18] H. He, M. Friese, N. Heckenberg, and H. Rubinsztein-Dunlop, "Direct observation of transfer of angular momentum to absorptive particles from a laser beam with a phase singularity," *Phys. Rev. Lett.*, vol. 75, no. 5, 1995, Art. no. 826.

[19] C. Zhang et al., "Orbital angular momentum detection device for vortex microwave photons," *Commun. Eng.*, vol. 2, no. 1, Mar. 2023, Art. no. 11, doi: 10.1038/s44172-023-00056-5.

[20] M. Golub, E. Kaganov, A. Kondorov, V. A. Soifer, and G. Usplen'ev, "Experimental investigation of a multibeam holographic optical element matched to Gauss-Laguerre modes," *Quantum Electron.*, vol. 26, no. 2, 1996, Art. no. 184.

[21] D. M. Fatkhiev et al., "Recent advances in generation and detection of orbital angular momentum optical beams–A review," *Sensors*, vol. 21, no. 15, 2021, Art. no. 4988. [Online]. Available: https://www.mdpi.com/1424-8220/21/15/4988

[22] P. Genevet, J. Lin, M. A. Kats, and F. Capasso, "Holographic detection of the orbital angular momentum of light with plasmonic photodiodes," *Nature Commun.*, vol. 3, no. 1, pp. 1–5, 2012.

[23] Q. Zhao, M. Dong, Y. Bai, and Y. Yang, "Measuring high orbital angular momentum of vortex beams with an improved multipoint interferometer," *Photon. Res.*, vol. 8, no. 5, pp. 745–749, May 2020. [Online]. Available: https://opg.optica.org/prj/abstract.cfm?URI=prj-8-5-745

[24] Y. Ren et al., "Adaptive optics compensation of multiple orbital angular momentum beams propagating through emulated atmospheric turbulence," *Opt. Lett.*, vol. 39, no. 10, pp. 2845–2848, May 2014. [Online]. Available: https://opg.optica.org/ol/abstract.cfmURI=ol-39-10-2845

[25] T. Doster and A. T. Watnik, "Machine learning approach to OAM beam demultiplexing via convolutional neural networks," *Appl. Opt.*, vol. 56, no. 12, pp. 3386–3396, Apr. 2017. [Online]. Available: https://opg.optica.org/ao/abstract.cfmURI=ao-56-12-3386

[26] H. Chang et al., "Adaptive optics compensation of orbital angular momentum beams with a modified Gerchberg–Saxton-based phase retrieval algorithm," *Opt. Commun.*, vol. 405, pp. 271–275, 2017. [Online]. Available: https://www.sciencedirect.com/science/article/pii/S003040181730723X

[27] J. Zhu, A. Wang, X. Liu, Y. Liu, Z. Zhang, and F. Gao, "Reconstructing the wave function through the momentum weak value," *Phys. Rev. A*, vol. 104, no. 3, 2021, Art. no. 032221.

[28] M. Yang et al., "Zonal reconstruction of photonic wavefunction via momentum weak measurement," *Laser Photon. Rev.*, vol. 14, no. 5, 2020, Art. no. 1900251. [Online]. Available: https://onlinelibrary.wiley.com/doi/abs/10.1002/lpor.201900251

[29] X. Qiu et al., "Precision phase estimation based on weak-value amplification," *Appl. Phys. Lett.*, vol. 110, no. 7, 2017, Art. no. 071105, doi: 10.1063/1.4976312.
[30] V. P. Lukin, P. A. Konyaev, and V. A. Sennikov, "Beam spreading of vortex beams propagating in turbulent atmosphere," *Appl. Opt.*, vol. 51, no. 10, pp. C84–C87, 2012.
[31] J. Vickers, M. Burch, R. Vyas, and S. Singh, "Phase and interference properties of optical vortex beams," *JOSA A*, vol. 25, no. 3, pp. 823–827, 2008.
[32] D. Xu, S. He, J. Zhou, S. Chen, S. Wen, and H. Luo, "Optical analog computing of two-dimensional spatial differentiation based on the brewster effect," *Opt. Lett.*, vol. 45, no. 24, pp. 6867–6870, Dec. 2020. [Online]. Available: https://opg.optica.org/ol/abstract.cfm?URI=ol-45-24-6867
[33] S. He, J. Zhou, S. Chen, W. Shu, H. Luo, and S. Wen, "Spatial differential operation and edge detection based on the geometric spin hall effect of light," *Opt. Lett.*, vol. 45, no. 4, pp. 877–880, Feb. 2020. [Online]. Available: https://opg.optica.org/ol/abstract.cfm?URI=ol-45-4-877
[34] A. Wang et al., "Optical differentiation based on weak measurements," *Opt. Lett.*, vol. 47, no. 15, pp. 3880–3883, 2022.
[35] X. Liu et al., "General scheme of differential imaging employing weak measurement," *Phys. Rev. A*, vol. 106, Aug. 2022, Art. no. 023518. [Online]. Available: https://link.aps.org/doi/10.1103/PhysRevA.106.023518
[36] J. Zhu, A. Wang, F. Gao, and Z. Zhang, "Realization of a sign-distinguishable higher-order optical differentiation," *Phys. Rev. A*, vol. 106, Aug. 2022, Art. no. 023516. [Online]. Available: https://link.aps.org/doi/10.1103/PhysRevA.106.023516
[37] X. Zhu, Y. Zhang, S. Pang, C. Qiao, Q. Liu, and S. Wu, "Quantum measurements with preselection and postselection," *Phys. Rev. A*, vol. 84, Nov. 2011, Art. no. 052111. [Online]. Available: https://link.aps.org/doi/10.1103/PhysRevA.84.052111
[38] F. Li, J. Huang, and G. Zeng, "Adaptive weak-value amplification with adjustable postselection," *Phys. Rev. A*, vol. 96, Sep. 2017, Art. no. 032112. [Online]. Available: https://link.aps.org/doi/10.1103/PhysRevA.96.032112
[39] A. M. Yao and M. J. Padgett, "Orbital angular momentum: Origins, behavior and applications," *Adv. Opt. Photon.*, vol. 3, no. 2, pp. 161–204, Jun. 2011. [Online]. Available: https://opg.optica.org/aop/abstract.cfmURI=aop-3-2-161
[40] J. Verbeeck, H. Tian, and P. Schattschneider, "Production and application of electron vortex beams," *Nature*, vol. 467, no. 7313, 2010, Art. no. 301.
[41] S. Mang-zuo, "Numerical simulation and validation of phase screen distorted by atmospheric turbulence," *Opto- Electron. Eng.*, vol. 34, pp. 1–4, 2007.
[42] I. Toselli, L. Andrews, R. Phillips, and V. Ferrero, "Free space optical system performance for laser beam propagation through non-Kolmogorov turbulence," *Opt. Eng.*, vol. 47, pp. 026003–026003, 2008.
[43] X. Liu, Y. Zhu, C. Chen, Z. Hu, and Y. Zhang, "Effects of atmospheric turbulence on the orbital angular momentum of multi-Gaussian Schell model beams," *Optik*, vol. 124, no. 24, pp. 6892–6895, 2013. [Online]. Available: https://www.sciencedirect.com/science/article/pii/S0030402613008279
[44] K. Yong, J. Yan, S. Huang, and R. Zhang, "Propagation characteristics of optical vortex pulse in atmospheric turbulence," *Optik*, vol. 180, pp. 27–33, 2019. [Online]. Available: https://www.sciencedirect.com/science/article/pii/S0030402618318175
[45] C. Paterson, "Atmospheric turbulence and orbital angular momentum of single photons for optical communication," *Phys. Rev. Lett.*, vol. 94, Apr. 2005, Art. no. 153901. [Online]. Available: https://link.aps.org/doi/10.1103/PhysRevLett.94.153901
[46] J. Sinclair, M. Hallaji, A. M. Steinberg, J. Tollaksen, and A. N. Jordan, "Weak-value amplification and optimal parameter estimation in the presence of correlated noise," *Phys. Rev. A*, vol. 96, Nov. 2017, Art. no. 052128. [Online]. Available: https://link.aps.org/doi/10.1103/PhysRevA.96.052128
[47] P. B. Dixon, D. J. Starling, A. N. Jordan, and J. C. Howell, "Ultrasensitive beam deflection measurement via interferometric weak value amplification," *Phys. Rev. Lett.*, vol. 102, Apr. 2009, Art. no. 173601. [Online]. Available: https://link.aps.org/doi/10.1103/PhysRevLett.102.173601
[48] L. Zhang, A. Datta, and I. A. Walmsley, "Precision metrology using weak measurements," *Phys. Rev. Lett.*, vol. 114, May 2015, Art. no. 210801. [Online]. Available: https://link.aps.org/doi/10.1103/PhysRevLett.114.210801
[49] B. Rodenburg et al., "Influence of atmospheric turbulence on states of light carrying orbital angular momentum," *Opt. Lett.*, vol. 37, no. 17, pp. 3735–3737, Sep. 2012. [Online]. Available: https://opg.optica.org/ol/abstract.cfm?URI=ol-37-17-3735
[50] B. B. Yousif, E. E. Elsayed, and M. M. Alzalabani, "Atmospheric turbulence mitigation using spatial mode multiplexing and modified pulse position modulation in hybrid RF/FSO orbital-angular-momentum multiplexed based on MIMO wireless communications system," *Opt. Commun.*, vol. 436, pp. 197–208, 2019. [Online]. Available: https://www.sciencedirect.com/science/article/pii/S0030401818310836
[51] B. B. Yousif and E. E. Elsayed, "Performance enhancement of an orbital-angular-momentum-multiplexed free-space optical link under atmospheric turbulence effects using spatial-mode multiplexing and hybrid diversity based on adaptive MIMO equalization," *IEEE Access*, vol. 7, pp. 84401–84412, 2019.
[52] Y. Shen et al., "Optical vortices 30 years on: OAM manipulation from topological charge to multiple singularities," *Light: Sci. Appl.*, vol. 8, no. 1, Oct. 2019, Art. no. 90, doi: 10.1038/s41377-019-0194-2.